Report on CCL Key Comparison
Measurement of optical polygons
CCL-K3.n01
Final Report

B. J. Eves (NRC), W. Shihua (NMC,A*STAR),
M del Mar Perez Hernandez (CEM), F. Huerta Yshikawa (CENAM),
L. H. B. Vieira (INMETRO), M. Astrua (INRIM), J. Y. Lee (KRISS),
Z. Xue (NIM), T. Watanabe (NMIJ), T. Yandayan (TUBITAK UME)

February 17, 2026

Contents

1 Document control

Version Draft A.1	Issued on 02 September 2025.
Version Draft A.2	Issued on 16 September 2025.
Version Draft A.3	Issued on 10 October 2025.
Version Draft A.4	Issued on 24 October 2025.
Version Draft B	Issued on 12 November 2025.
Version Draft B.1	Issued on 02 February 2026.
Version Final Report	Issued on 17 February 2026.

2 Introduction

The metrological equivalence of national measurement standards and of calibration certificates issued by national metrology institutes is established by a set of key and supplementary comparisons chosen and organized by the Consultative Committees of the CIPM or by the regional metrology organizations in collaboration with the Consultative Committees.

At its meeting in 2014, the Consultative Committee for Length (CCL) WG-MRA decided upon a key comparison on the measurement of angle standards with NMISA as the pilot Laboratory. The initial scope of the comparison included the calibration of polygons and angle encoders. After extensive discussion the scope was limited to polygon standards. In 2022 NMISA announced they could not continue as the pilot laboratory and NRC-CNRC volunteered to assume the role of pilot. The comparison was initially registered in 2020 with the identifier CCL-K3.2020, and was later renamed according to the revised naming scheme as CCL-K3.n01. Artefact circulation was started in April 2023, and was completed in September 2025.

3 Organization

3.1 Participants

Table 1: List of participant laboratories and their contacts.

Lab Code	Institute and address	Contact person, phone, email
NMC, A*STAR	National Metrology Centre 8 CleanTech Loop Unit 01-20 Singapore 637145	**Wang Shihua** +65 6714 9264 wang.shihua@nmc.a-star.edu.sg
CEM	Centro Español de Metrología Alfar 2, 28760 Tres Cantos, Madrid España	**M del Mar Perez Hernandez** +34 91 8074716 mmperezh@cem.es

continued on next page

Lab Code	Institute and address	Contact person, phone, email
CENAM	km 4,5 Carretera de los Cué El Margués, Queretaro México	**Carlos Alberto Galván Hernandez** +52 442 2110500 Ext. 3295 cgalvan@cenam.mx **Francisco Huerta Yshikawa** +52 442 2110500 Ext. 3283 fhuerta@cenam.mx
INMETRO	National Institute of Metrology, Quality and Technology Av. N. Sra. das Gra$\mathbf{x}_c$as, 50 Xerém - Duque de Caxias - RJ 20.250-020 - Brazil	**Luiz Henrique Brum Vieira** +55 21 2679 9020/9024 lhvieira@inmetro.gov.br
INRIM	Istituto Nazionale di Ricerca Metrologica str. delle cacce, 91 10135 Torino Italia	**Marco Pisani** +39 011 3919 966 m.pisani@inrim.it **Milena Astrua** +39 011 3919 963 m.astrua@inrim.it
KRISS	Korea Research Institute of Standards and Science 267 Gajeong-ro Yuseong-gu, Daejeon 34113, Republic of Korea	**Yae Yong Lee** +82 42 868 5226 +82 10 5431 8690 (mobile) jaeyong@kriss.re.kr
NIM	National Institute of Metrology No. 18, Bei San Huan Dong Lu Chaoyang District Beijing 100029 P. R. of China	**Zi Xue** +86 10 64524916 xuez@nim.ac.cn
NMIJ	National Metrology Institute of Japan National Institute of Advanced Industrial Science and Technology Central3 1-1-1 Umezono, Tsukuba, Ibaraki, 3058563, Japan	**Tsukasa Watanabe** +81 29 8614291 t.watanabe@aist.go.jp
NRC-CNRC	Metrology National Research Council Canada 1200 Montreal Road, building M-36 Ottawa, ON K1A 0R6, Canada	**Brian J. Eves** +1 613 991 3279 brian.eves@nrc-cnrc.gc.ca
TUBITAK UME	Dimensional Group Labs TÜBİTAK Gebze Yerleşkesi	**Tanfer Yandayan** +90 262 679 5000 ext. 5312

continued on next page

Lab Code	Institute and address	Contact person, phone, email
	Baris Mah. Dr. Zeki Acar Cad. No:1 41470 Gebze KOCAELİ Turkey	tanfer.yandayan@tubitak.gov.tr **S. Asli Akgoz** +90 262 679 5000 ext. 5301 asli.akgoz@tubitak.gov.tr

3.2 Schedule

Table 2: List of initial participant laboratory schedule, the actual date of measurement, and the date the results were received.

RMO	Laboratory	Original schedule	Date of measurement	Results received
SIM	NRC-CNRC	2023-03-01	2023-03-32	-
EURAMET	INRIM	2023-05-24	2023-06-05	2023-10-23
APMP	NIM	2023-07-05	2023-07-19	2023-11-09
APMP	NMIJ	2023-08-16	2023-09-13	2023-12-13
SIM	CENAM	2023-09-27	2023-11-06	2024-01-16
SIM	NRC-CNRC	2023-10-08	2024-02-14	-
EURAMET	TUBITAK UME	2023-12-20	2024-05-05	2024-09-29
EURAMET	CEM	2024-01-31	2024-09-03	2024-12-02
APMP	KRISS	2024-03-13	2024-11-26	2025-01-08
SIM	INMETRO	2024-04-24	2025-08-01	2025-08-20
APMP	NMC,A*STAR	2024-06-05	2025-03-25	2025-03-25
SIM	NRC-CNRC	2024-07-17	2025-08-30	-

4 Artefacts

4.1 Description of artefacts

The 10-sided polygon, serial number 31391.15, is manufactured by Starrett-Webber and is made of chrome carbide. The measuring faces have a rectangular cross-section of approximately 14 mm by 16 mm. The polygon has a center hole of 25.4 mm for mounting and a height of 17.5 mm. The normal orientation of the polygon is defined as the orientation in which the face numbers are visible on the top surface of the polygon. The inverted orientation has the serial number visible on the top surface of the polygon. The polygon is shown on the right-hand side of figure 1.

The 12-sided polygon, serial number 327, is manufactured by Möller-Wedel and comprises a low coefficient of thermal expansion glass polygon mounted upon a stainless steel base. The measuring faces have a diameter of approximating 25 mm. The polygon has a center hole of 16 mm for mounting and a

height of 60 mm. The polygon should only be measured in the normal orientation, i.e. with the steel base plate below the Zerodur component. The polygon is shown on the left-hand side of figure 1.

Each polygon has n internal angle measurands where n is the number of faces of the polygon. The measurands are labeled according to the face numbers using the following scheme: i:$(i+1)$ represents the internal angle between face i and face $i+1$. For example, the measurand labels for a four sided polygon would be 1:2, 2:3, 3:4, and 4:1.

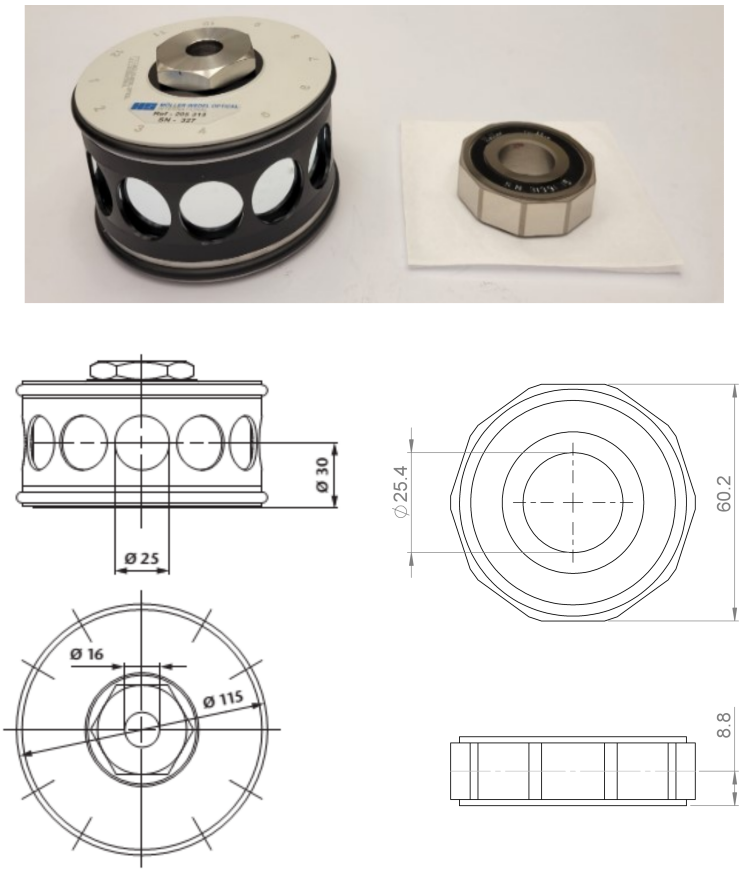

Figure 1: Comparison artifacts. Units are in mm.

4.2 Stability of artefacts

NRC-CNRC measured the artefacts three times over the course of the comparison: at the start, middle, and end. The stability of the 10-sided polygon, serial number 31391.15, is shown in figure 2. The internal angles for the polygon are shown with the Key Comparison Reference Values (KCRV) (calculated

in section 7.1) subtracted, and the internal angles have been offset from each other along the horizontal axis for clarity. The pooled standard deviation for all internal angles is 0.008 arcsecond which is less than the NRC-CNRC standard uncertainty of 0.028 arcsecond, and there is no evidence for artifact instability.

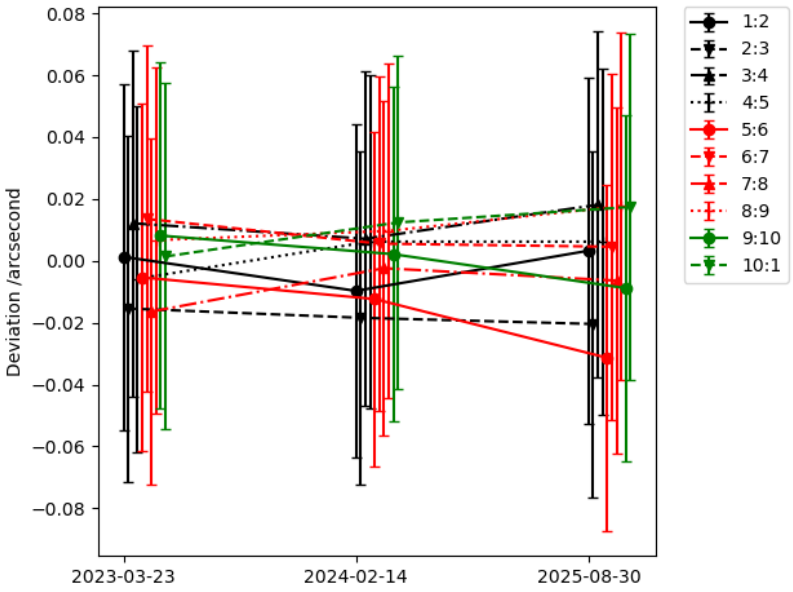

Figure 2: Stability measurements for the 10 sided polygon with serial number 31391.15. The pooled standard deviation for all faces is 0.008 arcsecond. The points for each internal angle have been horizontally offset for clarity and the KCRV values subtracted.

The stability of the 12-sided polygon, serial number 327, is shown in figure 3. The internal angles for the polygon are once again shown with the KCRV values (calculated in section 7.1) subtracted, and the internal angles have been offset from each other along the horizontal axis for clarity. The pooled standard deviation for all internal angles is 0.079 arcsecond which is greater than the NRC-CNRC standard uncertainty of 0.033 arcsecond for this polygon. The 12-sided polygon was not stable for the duration of the comparison, and the instability is not a linear trend. NRC-CNRC has prior evidence that this kind of polygon can be sensitive to thermal fluctuations and we account for this instability by adding an additional uncertainty component equal to the pooled standard deviation of the stability measurements in quadrature with each NMI's reported uncertainty.

4.3 Condition of artefacts at start/end of the comparison

CENAM reported, after their measurements were complete on December 12$^{\text{th}}$ 2023, that the 12-sided polygon had finger prints on faces 1, 3, 4, 7, 8, 11,

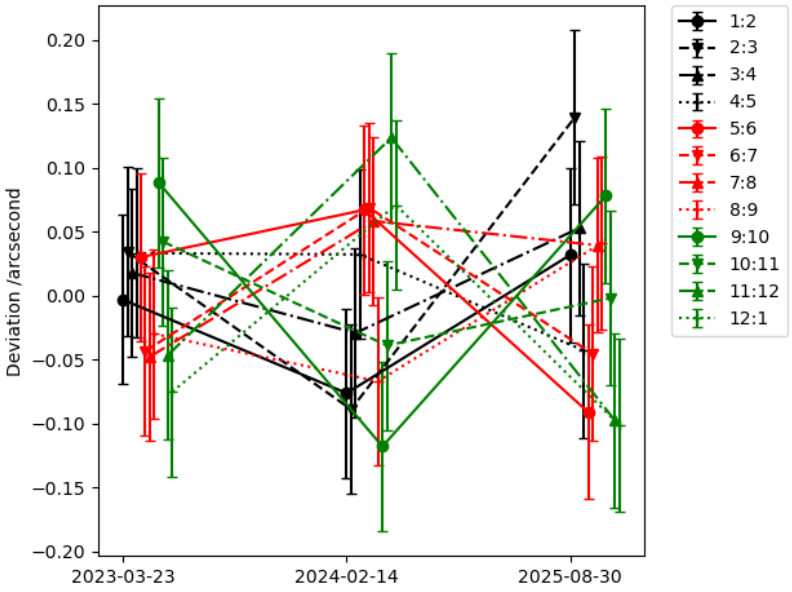

Figure 3: Stability measurements for the 12 sided polygon with serial number 327. The pooled standard deviation for all faces is 0.079 arcsecond. The points for each internal angle have been horizontally offset for clarity and the KCRV values subtracted.

and 12. To properly remove the finger prints the steel mask cyclinder which surrounds the optical polygon would need to be removed. The potential for a non-reversible change to the polygon measurands during the finger print cleaning was considered to be too high and the finger prints were left as is. Note that the finger prints did not compromise the ability of any of the NMIs from measuring the polygon angles. The stability of the artefact, shown in figure 3, shows no obvious change due to the presence of the finger prints. Shown in figure 4 is the damage reported for face 4 which is the largest print of those reported.

The 10-sided polygon also had finger prints observed on the faces at various points during the comparison. The material and construction of the polygon enabled the various laboratories to clean the faces using typical solvents.

Figure 4: Face 4 of the 12-sided polygon with serial number 327. A large finger print dominates the mirror surface.

5 Measuring instructions

5.1 Measurands

The polygons shall be measured based on the standard procedure that the laboratory regularly uses for this calibration service for its customers.

The measurand to be reported for the polygons is the pitch angles between the projections of two adjacent surface normals N_{i-1} and N_i in the measuring plane with the face counting index ($i = 1, 2, \ldots, n$). See figure 5. The deviations of the pitch angles from their nominal values of $360/n$ are referred to as pitch angle deviations, or

$$\Delta\alpha_i = \alpha_i - \frac{360}{n}. \tag{1}$$

The positive count direction of the polygon angle corresponds to the count direction of the face index i indicated on the polygon. In ideal conditions the

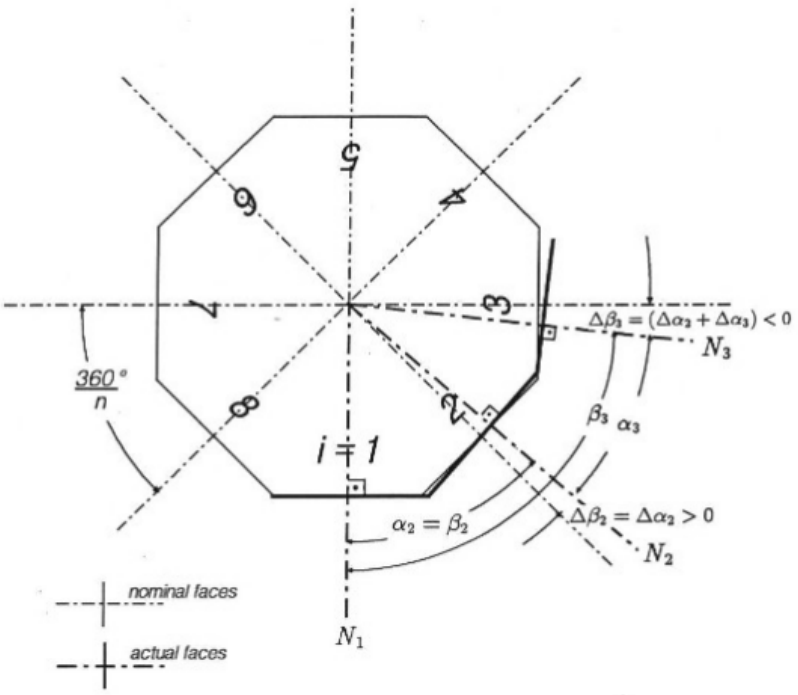

Figure 5: Definition of pitch angle and pitch angle deviations.

individual measuring faces are perpendicular to the measuring plane. In practice, the measuring faces are not perpendicular to the measuring plane by small tilts referred to as pyramidal errors. In that case, the measuring plane is defined as the plane for which the sum of the squares of the pyramidal errors of all measuring faces is a minimum.

The measurand definition for the plane angle of a single polygon face is the component of the average surface normal of the mirrored surface under the assumption of uniform light intensity that lies within the measuring plane. The entire surface of the target polygon face, i.e. no masking other than that intrinsically provided by the polygon, shall contribute to the average surface normal.

6 Results

6.1 Results and standard uncertainties as reported by participants

The results and standard uncertainties as reported by the participants for the 10-sided polygon with serial number 31391.15 are shown in tables 3 and 4. While

the results and standard uncertainties for the 12-sided polygon with serial number 327 are shown in tables 5 and 6. The NRC-CRNC, as pilot, has contributed four separate measurements over the course of the comparison. Three of the measurements comprise the stability check, and only the first measurement of these is used to determine the KCRV. The fourth measurement is via the angle interferometer that, in addition to measuring the polygon angles, is used to measure the surface flatness of the mirrored polygon faces. The angle interferometer measurements (labeled NRC-CNRC AI) were measured during the same period as the intial NRC-CNRC measurements, and do not contribute to the KCRV.

Table 3: Submitted results for the 10-sided polygon with serial number 31391.15. Values are in arcseconds.

NMI	1:2	2:3	3:4	4:5	5:6
NRC-CNRC	−0.360	−0.076	0.110	−0.570	0.689
NRC-CNRC AI	−0.375	−0.071	0.115	−0.568	0.685
INRIM	−0.362	−0.048	0.093	−0.587	0.711
NIM	−0.368	−0.051	0.088	−0.561	0.697
NMIJ	−0.368	−0.050	0.099	−0.556	0.698
CENAM	−0.360	−0.060	0.090	−0.560	0.710
NRC-CNRC	−0.371	−0.079	0.105	−0.558	0.682
TUBITAK UME	−0.360	−0.064	0.109	−0.578	0.696
CEM	−0.370	−0.060	0.090	−0.580	0.700
KRISS	−0.376	−0.065	0.113	−0.560	0.678
NMC,A*STAR	−0.080	−0.070	0.030	−0.090	0.120
INMETRO	−0.240	−0.160	0.040	−0.510	0.700
NRC-CNRC	−0.358	−0.081	0.116	−0.558	0.663

NMI	6:7	7:8	8:9	9:10	10:1
NRC-CNRC	−0.298	0.130	−0.151	0.078	0.448
NRC-CNRC AI	−0.312	0.139	−0.145	0.079	0.454
INRIM	−0.318	0.161	−0.163	0.071	0.443
NIM	−0.309	0.144	−0.164	0.079	0.447
NMIJ	−0.316	0.151	−0.163	0.064	0.445
CENAM	−0.330	0.130	−0.140	0.080	0.450
NRC-CNRC	−0.306	0.144	−0.148	0.072	0.459
TUBITAK UME	−0.322	0.185	−0.175	0.076	0.434
CEM	−0.320	0.140	−0.130	0.070	0.450
KRISS	−0.315	0.152	−0.147	0.060	0.460
NMC,A*STAR	−0.030	0.010	−0.010	−0.010	0.110
INMETRO	−0.360	0.170	−0.140	−0.040	0.530
NRC-CNRC	−0.307	0.140	−0.140	0.061	0.464

Table 4: Submitted standard uncertainties for the 10-sided polygon with serial number 31391.15. Values are in arcseconds.

NMI	1:2	2:3	3:4	4:5	5:6
NRC-CNRC	0.028	0.028	0.028	0.028	0.028
NRC-CNRC AI	0.024	0.024	0.024	0.024	0.024
INRIM	0.035	0.035	0.035	0.035	0.035
NIM	0.031	0.031	0.031	0.031	0.031
NMIJ	0.030	0.030	0.023	0.031	0.038
CENAM	0.050	0.050	0.050	0.050	0.050
NRC-CNRC	0.027	0.027	0.027	0.027	0.027
TUBITAK UME	0.060	0.060	0.060	0.060	0.060
CEM	0.080	0.080	0.080	0.080	0.080
KRISS	0.053	0.054	0.053	0.053	0.053
NMC,A*STAR	0.200	0.200	0.200	0.200	0.200
INMETRO	0.100	0.100	0.100	0.100	0.100
NRC-CNRC	0.028	0.028	0.028	0.028	0.028

NMI	6:7	7:8	8:9	9:10	10:1
NRC	0.028	0.028	0.028	0.028	0.028
NRC AI	0.024	0.024	0.024	0.024	0.024
INRIM	0.035	0.035	0.035	0.035	0.035
NIM	0.031	0.031	0.031	0.031	0.031
NMIJ	0.033	0.025	0.020	0.024	0.026
CENAM	0.050	0.050	0.050	0.050	0.050
NRC	0.027	0.027	0.027	0.027	0.027
TUBITAK UME	0.060	0.060	0.060	0.060	0.060
CEM	0.080	0.080	0.080	0.080	0.080
KRISS	0.054	0.053	0.054	0.053	0.053
NMC,A*STAR	0.200	0.200	0.200	0.200	0.200
INMETRO	0.100	0.100	0.100	0.100	0.100
NRC	0.028	0.028	0.028	0.028	0.028

Table 5: Submitted results for the polygon with serial number 327. Values are in arcseconds.

NMI	1:2	2:3	3:4	4:5	5:6	6:7
NRC-CNRC	−0.297	−0.655	−0.464	−0.274	0.371	0.504
NRC-CNRC AI	−0.298	−0.642	−0.495	−0.269	0.359	0.503
INRIM	−0.306	−0.669	−0.458	−0.276	0.336	0.510
NIM	−0.216	−0.707	−0.580	−0.356	0.372	0.599
NMIJ	−0.428	−0.783	−0.444	−0.265	0.419	0.591
CENAM	−0.390	−0.760	−0.450	−0.270	0.370	0.580
NRC-CNRC	−0.370	−0.778	−0.511	−0.275	0.408	0.616
TUBITAK UME	−0.236	−0.656	−0.499	−0.334	0.303	0.538
CEM	−0.200	−0.670	−0.520	−0.380	0.280	0.530
KRISS	−0.241	−0.672	−0.507	−0.352	0.305	0.561
NMC,A*STAR	−0.280	−0.340	−0.280	−0.190	0.200	0.370
INMETRO	−0.200	−0.590	−0.450	−0.340	0.220	0.500
NRC-CNRC	−0.262	−0.550	−0.429	−0.350	0.250	0.502

NMI	7:8	8:9	9:10	10:11	11:12	12:1
NRC-CNRC	0.200	−0.003	0.161	−0.566	0.169	0.852
NRC-CNRC AI	0.228	−0.018	0.168	−0.569	0.178	0.857
INRIM	0.189	0.037	0.178	−0.558	0.174	0.843
NIM	0.288	0.028	0.001	−0.644	0.220	0.996
NMIJ	0.207	−0.023	−0.028	−0.550	0.350	0.956
CENAM	0.220	−0.050	−0.020	−0.550	0.350	0.960
NRC-CNRC	0.306	−0.040	−0.045	−0.647	0.339	0.998
TUBITAK UME	0.293	0.092	0.106	−0.700	0.134	0.959
CEM	0.300	0.070	0.110	−0.720	0.170	1.030
KRISS	0.339	0.082	0.090	−0.737	0.144	0.986
NMC,A*STAR	0.090	0.070	−0.010	−0.060	0.000	0.430
INMETRO	0.290	0.090	0.120	−0.640	0.160	0.850
NRC-CNRC	0.287	0.068	0.151	−0.610	0.118	0.826

Table 6: Submitted standard uncertainties for the 12-sided polygon with serial number 327. Values are in arcseconds.

NMI	1:2	2:3	3:4	4:5	5:6	6:7
NRC-CNRC	0.033	0.033	0.033	0.033	0.033	0.033
NRC-CNRC AI	0.024	0.024	0.024	0.024	0.024	0.024
INRIM	0.039	0.039	0.039	0.039	0.039	0.039
NIM	0.040	0.040	0.040	0.040	0.040	0.040
NMIJ	0.023	0.025	0.031	0.035	0.036	0.035
CENAM	0.040	0.040	0.040	0.040	0.040	0.040
NRC-CNRC	0.033	0.033	0.033	0.033	0.033	0.033
TUBITAK UME	0.060	0.060	0.060	0.060	0.060	0.060
CEM	0.090	0.090	0.090	0.090	0.090	0.100
KRISS	0.053	0.054	0.053	0.058	0.053	0.053
NMC,A*STAR	0.250	0.250	0.250	0.250	0.250	0.250
INMETRO	0.100	0.100	0.100	0.100	0.100	0.100
NRC-CNRC	0.034	0.034	0.034	0.034	0.034	0.034

NMI	7:8	8:9	9:10	10:11	11:12	12:1
NRC-CNRC	0.033	0.033	0.033	0.033	0.033	0.033
NRC-CNRC AI	0.024	0.024	0.024	0.024	0.024	0.024
INRIM	0.039	0.039	0.039	0.039	0.039	0.039
NIM	0.040	0.040	0.040	0.040	0.040	0.040
NMIJ	0.029	0.031	0.032	0.026	0.024	0.024
CENAM	0.040	0.040	0.040	0.040	0.040	0.040
NRC-CNRC	0.033	0.033	0.033	0.033	0.033	0.033
TUBITAK UME	0.060	0.060	0.060	0.060	0.060	0.060
CEM	0.100	0.120	0.100	0.100	0.090	0.100
KRISS	0.053	0.052	0.053	0.059	0.054	0.056
NMC,A*STAR	0.250	0.250	0.250	0.250	0.250	0.250
INMETRO	0.100	0.100	0.100	0.100	0.100	0.100
NRC-CNRC	0.034	0.034	0.034	0.034	0.034	0.034

Table 7: Comparison of the range of submitted standard uncertainties and the published standard uncertainty CMC values. All values are in units of arcseconds.

Laboratory	Standard uncertainty range	Standard uncertainty CMC
NRC-CNRC	0.028 to 0.033	0.031
INRIM	0.035 to 0.039	0.035
NIM	0.031 to 0.040	0.045
NMIJ	0.020 to 0.038	0.045
CENAM	0.04 to 0.05	–
TUBITAK UME	0.06	0.06
CEM	0.08 to 0.12	0.075 to 0.125
KRISS	0.052 to 0.059	0.055
INMETRO	0.1	0.15
NMC,A*STAR	0.20 to 0.25	0.25

6.2 Measurement uncertainties

The range of measurement uncertainties ($k = 1$) claimed by the participants and their standard uncertainty CMC claims are shown in table 7.

7 Analysis

7.1 Calculation of the KCRV

For a total number of participants, I, the normalized weight, w_i, for the result x_i and associated standard uncertainty $u(x_i)$ is

$$w_i = C \cdot \frac{1}{\left[u\left(x_i\right)\right]^2}, \tag{2}$$

where the normalising factor, C, is given by

$$C = \frac{1}{\sum_{i=1}^{I} \left[\frac{1}{u(x_i)}\right]^2}. \tag{3}$$

The weighted mean, $\overline{x_w}$, or the KCRV, is equal to

$$\overline{x_w} = \sum_{i=1}^{I} w_i \cdot x_i, \tag{4}$$

and the uncertainty of the weighted mean is calculated with

$$u\left(\overline{x_w}\right) = \sqrt{\frac{1}{\sum_{i=1}^{I} \left[\frac{1}{u(x_i)}\right]^2}} = \sqrt{C}. \tag{5}$$

If a laboratory's results contributed to the weighted mean [1] (and is therefore correlated to it) then the uncertainty of the difference between the result of a laboratory and the weighted mean is given by

$$u\left(x_i - \overline{x_w}\right) = \sqrt{u^2(x_i) - u^2(\overline{x_w})}. \tag{6}$$

If, on the other hand, a laboratory's results did not contribute to the weighted mean then the uncertainty of the difference between the results of a laboratory and the weighted mean is given by

$$u\left(x_i - \overline{x_w}\right) = \sqrt{u^2(x_i) + u^2(\overline{x_w})}. \tag{7}$$

The normalized error, E_n, between a laboratory's results and the KCRV value is used to measure the degree of agreement of the results contributing to the KCRV. It is defined as the ratio of the deviation from the weighted mean, divided by the expanded uncertainty of the deviation or

$$E_n = \frac{x_i - \overline{x_w}}{U\left(x_i - \overline{x_w}\right)} \tag{8}$$

where either equations 6 or 7 is used depending on whether the laboratoy result contributed to the KCRV value. If the $|E_n| > 1$ then the measurement result is potentially in disagreement with the KCRV.

The Birge ratio, R_B, is used to check that the distribution of E_n values for a particular KCRV value is statistically consistent. It is calculated by

$$R_B = \frac{u_{\text{ext}}(\overline{x_w})}{u(\overline{x_w})}, \tag{9}$$

where $u_{\text{ext}}(\overline{x_w})$ is the external standard deviation or

$$u_{\text{ext}}(\overline{x_w}) = \sqrt{\frac{1}{I-1} \cdot \frac{\sum_{i=1}^{I} w_i (x_i - \overline{x_w})^2}{\sum_{i=1}^{I} w_i}}. \tag{10}$$

The data is consistent within a 95% confidence limit if

$$R_B < \sqrt{1 + \sqrt{8/(I-1)}}. \tag{11}$$

In the event that the data is inconsistent a laboratory (likely the one with the largest $|E_n|$ value greater than one) is removed from the calculation of the KCRV. The KCRV and the Birge ratio are recalculated, and the process repeated until the Birge limit is satisfied for the largest possible set of contributing laboratories [2].

The KCRV values, and the calculated Birge ratios are shown in table 8 for the 10-sided polygon (serial number 31391.15), and in table 9 for the 12-sided polygon (serial number 327). As discussed in section 4.2 the particpant laboratories uncertainties have been increased by the artefact uncertainty (sum of squares) in order to account for artefact instability for the 12-sided polygon (see appendix A for analysis of the results without the inclusion of the artefact uncertainty). No laboratory's were removed from the calculation of the KCRV values.

Table 8: KCRV values, Birge ratios, and associated Birge limits for polygon 31391.15. Angle values are in arcseconds.

Angle	Value	$U(k=1)$	R_B	R_B Limit
1:2	−0.361	0.013	0.64	1.39
2:3	−0.061	0.013	0.43	1.39
3:4	0.098	0.013	0.32	1.39
4:5	−0.564	0.013	0.85	1.39
5:6	0.694	0.014	0.98	1.39
6:7	−0.312	0.014	0.55	1.39
7:8	0.146	0.013	0.42	1.39
8:9	−0.158	0.012	0.36	1.39
9:10	0.070	0.013	0.43	1.39
10:1	0.447	0.013	0.64	1.39

Table 9: KCRV values, Birge ratios, and associated Birge limits for polygon 327. Angle values are in arcseconds.

Angle	Value	$U(k=1)$	R_B	R_B Limit
1:2	−0.294	0.031	0.85	1.39
2:3	−0.689	0.031	0.73	1.39
3:4	−0.482	0.031	0.53	1.39
4:5	−0.307	0.031	0.46	1.39
5:6	0.341	0.031	0.57	1.39
6:7	0.547	0.031	0.45	1.39
7:8	0.248	0.031	0.59	1.39
8:9	0.027	0.032	0.51	1.39
9:10	0.073	0.031	0.83	1.39
10:11	−0.608	0.031	1.03	1.39
11:12	0.216	0.031	0.93	1.39
12:1	0.927	0.031	0.92	1.39

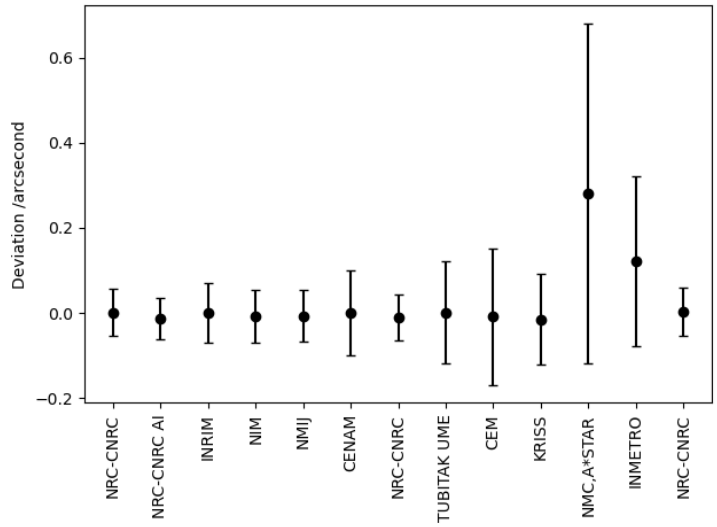

Figure 6: Angle 1:2 for polygon 31391.15. Error bars are $U(k = 2)$.

7.2 Calculation of degrees of equivalence

The degrees of equivalence for the measurement results are reported using the normalized errors as shown in tables 10 and 11 for the 10-sided polygon (serial number 31391.15) and the 12-sided polygon (serial number 327). Measurements which exceed $|E_n| > 1$ are highlighted in red.

7.3 Graphical representation of results

The differences between the participants measurement results and the KCRV values are shown in figures 6 through 27.

7.4 Discussion

The measurement results for the 10-sided polygon (serial number 31391.15) are excellent. The normalized error for the vast majority of laboratories does not exceed 0.3 and as a group we appear to be conservative in our uncertainty estimation.

The measurement results for the 12-sided polygon (serial number 327) are less positive. The transportation of the polygon was problematic due to the difficulty in cleaning the mirror faces after finger print contamination. Note that the 10-sided polygon also acquired finger prints during the comparison but they could easily be cleaned. The biggest issue, however, was the lack of stability of the artefact which did not appear to be influenced by the presence of the finger prints. NRC believes the instability is related to the construction of the

Table 10: E_n values for the 10-sided polygon with serial number 31391.15.

NMI	1:2	2:3	3:4	4:5	5:6
NRC-CNRC	0.03	−0.31	0.24	−0.12	−0.11
NRC-CNRC AI	−0.25	−0.19	0.32	−0.07	−0.17
INRIM	−0.01	0.19	−0.07	−0.35	0.26
NIM	−0.12	0.17	−0.17	0.06	0.05
NMIJ	−0.13	0.20	0.03	0.15	0.05
CENAM	0.01	0.01	−0.08	0.04	0.16
NRC-CNRC	−0.16	−0.31	0.12	0.10	−0.20
TUBITAK UME	0.01	−0.03	0.09	−0.12	0.01
CEM	−0.06	0.00	−0.05	−0.10	0.04
KRISS	−0.14	−0.04	0.15	0.04	−0.16
NMC,A*STAR	0.70	−0.02	−0.17	1.19	-1.44
INMETRO	0.61	−0.50	−0.29	0.27	0.03
NRC-CNRC	0.05	−0.33	0.30	0.10	−0.50

NMI	6:7	7:8	8:9	9:10	10:1
NRC-CNRC	0.28	−0.33	0.13	0.16	0.03
NRC-CNRC AI	−0.01	−0.14	0.24	0.17	0.14
INRIM	−0.10	0.22	−0.08	0.02	−0.06
NIM	0.05	−0.04	−0.11	0.16	0.01
NMIJ	−0.07	0.11	−0.17	−0.14	−0.04
CENAM	−0.19	−0.17	0.18	0.10	0.04
NRC-CNRC	0.09	−0.04	0.16	0.04	0.21
TUBITAK UME	−0.09	0.33	−0.15	0.05	−0.11
CEM	−0.05	−0.04	0.17	0.00	0.02
KRISS	−0.03	0.05	0.10	−0.10	0.13
NMC,A*STAR	0.71	−0.34	0.37	−0.20	−0.84
INMETRO	−0.24	0.12	0.09	−0.55	0.42
NRC-CNRC	0.07	−0.10	0.29	−0.14	0.28

Table 11: E_n values for the 12-sided polygon with serial number 327.

NMI	1:2	2:3	3:4	4:5	5:6	6:7
NRC-CNRC	−0.02	0.22	0.11	0.21	0.19	−0.27
NRC-CNRC AI	−0.02	0.27	−0.07	0.22	0.10	−0.25
INRIM	−0.07	0.12	0.15	0.19	−0.03	−0.23
NIM	0.47	−0.11	−0.60	−0.30	0.19	0.31
NMIJ	−0.89	−0.61	0.24	0.26	0.48	0.27
CENAM	−0.58	−0.43	0.19	0.23	0.18	0.20
NRC-CNRC	−0.42	−0.49	−0.16	0.18	0.37	0.38
TUBITAK UME	0.31	0.18	−0.09	−0.14	−0.20	−0.05
CEM	0.41	0.08	−0.17	−0.32	−0.26	−0.07
KRISS	0.30	0.10	−0.14	−0.24	−0.20	0.08
NMC,A*STAR	0.03	0.67	0.39	0.23	−0.27	−0.34
INMETRO	0.38	0.40	0.13	−0.13	−0.49	−0.19
NRC-CNRC	0.17	0.76	0.29	−0.23	−0.50	−0.25

NMI	7:8	8:9	9:10	10:11	11:12	12:1
NRC-CNRC	−0.30	−0.19	0.56	0.27	−0.29	−0.47
NRC-CNRC AI	−0.11	−0.25	0.54	0.22	−0.21	−0.40
INRIM	−0.36	0.06	0.64	0.31	−0.25	−0.51
NIM	0.24	0.01	−0.44	−0.22	0.03	0.42
NMIJ	−0.26	−0.32	−0.64	0.38	0.88	0.19
CENAM	−0.17	−0.47	−0.56	0.35	0.82	0.20
NRC-CNRC	0.32	−0.37	−0.65	−0.21	0.68	0.39
TUBITAK UME	0.24	0.35	0.18	−0.49	−0.43	0.17
CEM	0.21	0.15	0.15	−0.45	−0.20	0.42
KRISS	0.51	0.31	0.10	−0.69	−0.40	0.32
NMC,A*STAR	−0.30	0.08	−0.16	1.05	−0.41	−0.96
INMETRO	0.17	0.26	0.19	−0.13	−0.23	−0.31
NRC-CNRC	0.22	0.23	0.43	−0.01	−0.54	−0.55

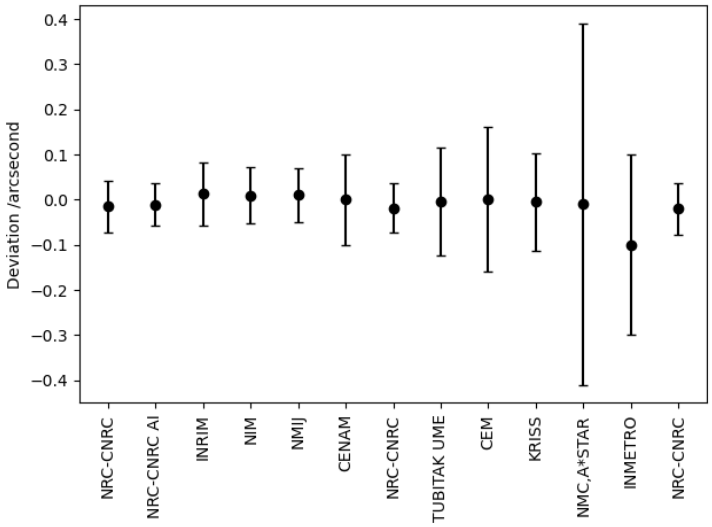

Figure 7: Angle 2:3 for polygon 31391.15. Error bars are $U(k = 2)$.

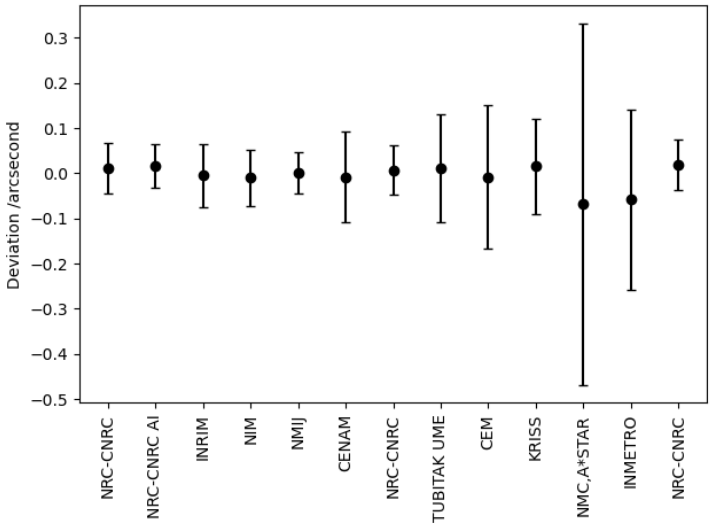

Figure 8: Angle 3:4 for polygon 31391.15. Error bars are $U(k = 2)$.

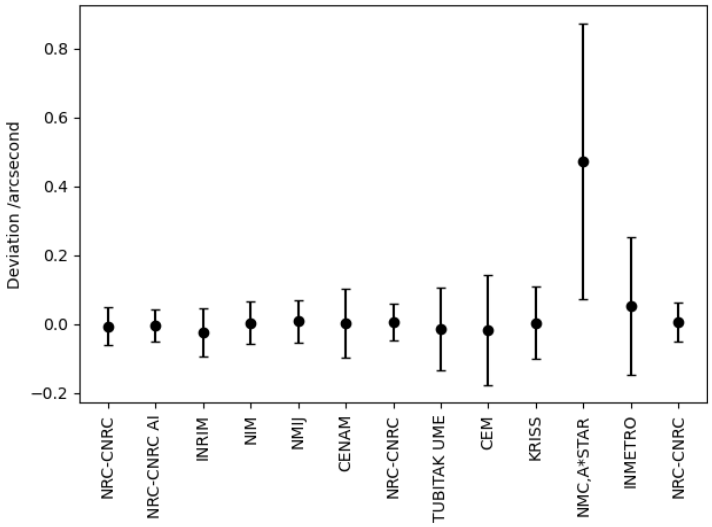

Figure 9: Angle 4:5 for polygon 31391.15. Error bars are $U(k = 2)$.

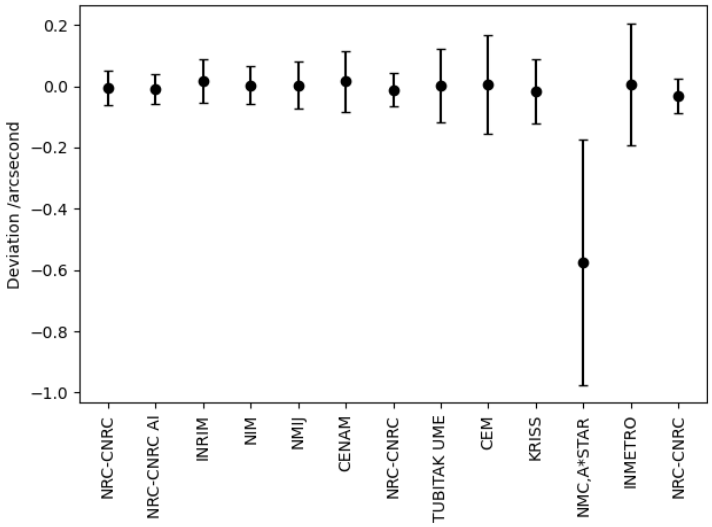

Figure 10: Angle 5:6 for polygon 31391.15. Error bars are $U(k = 2)$.

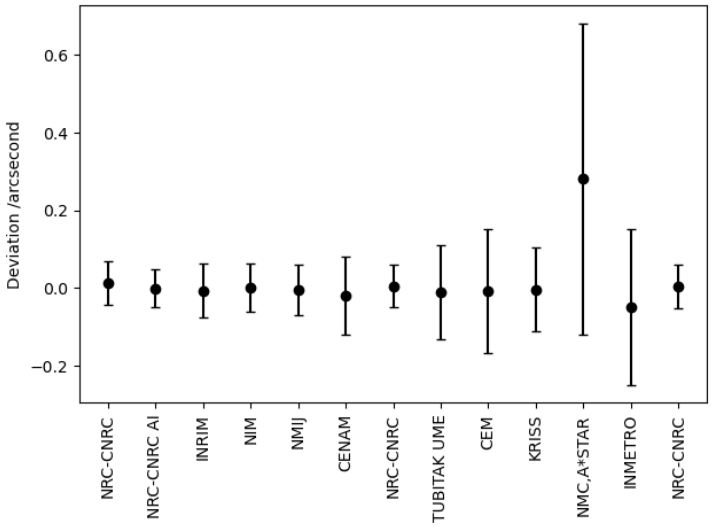

Figure 11: Angle 6:7 for polygon 31391.15. Error bars are $U(k = 2)$.

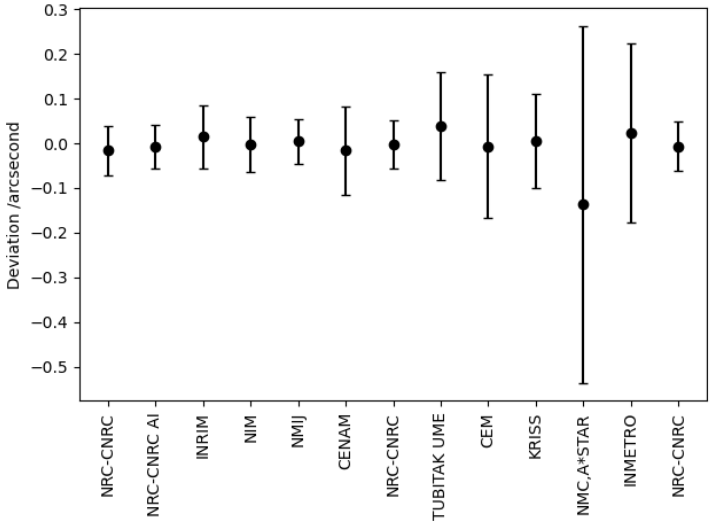

Figure 12: Angle 7:8 for polygon 31391.15. Error bars are $U(k = 2)$.

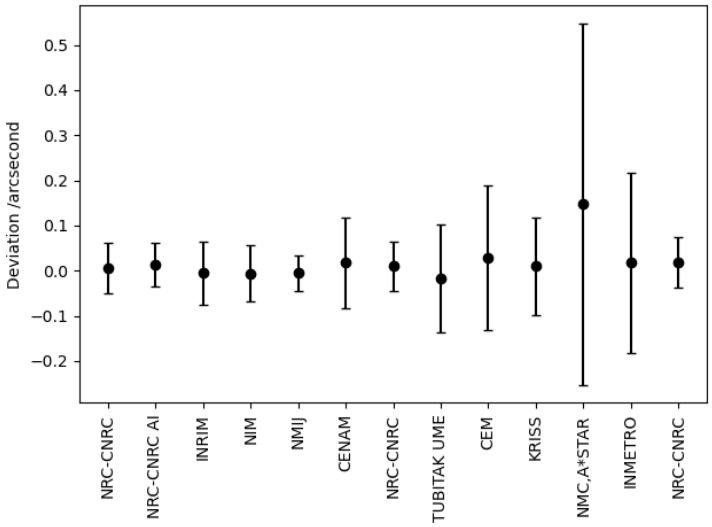

Figure 13: Angle 8:9 for polygon 31391.15. Error bars are $U(k = 2)$.

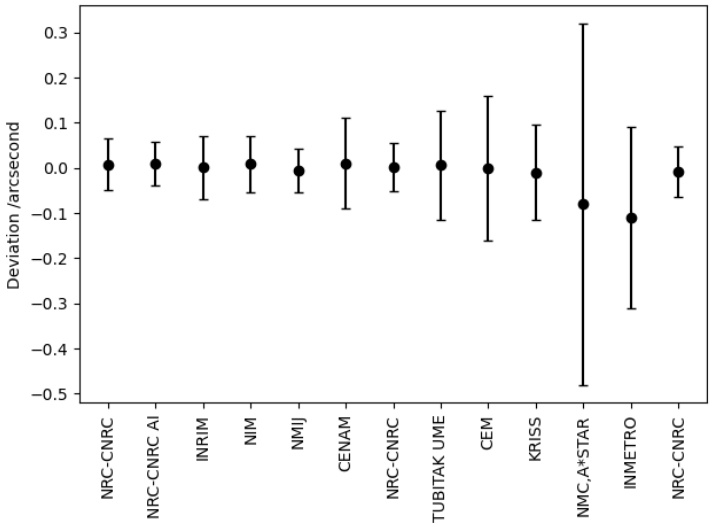

Figure 14: Angle 9:10 for polygon 31391.15. Error bars are $U(k = 2)$.

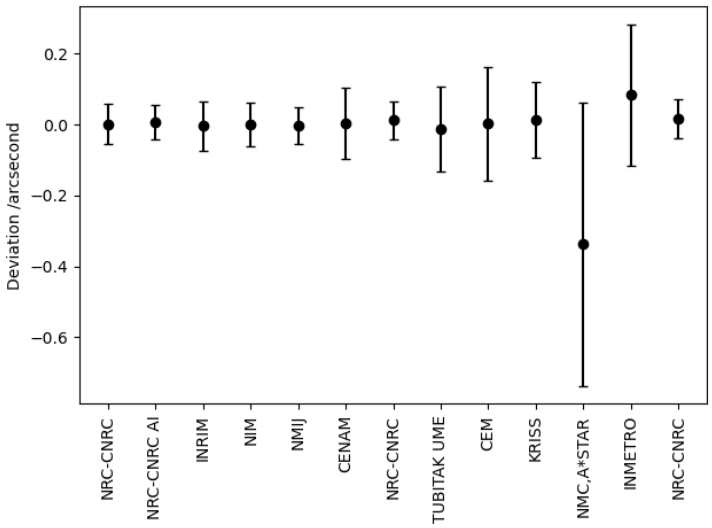

Figure 15: Angle 10:1 for polygon 31391.15. Error bars are $U(k = 2)$.

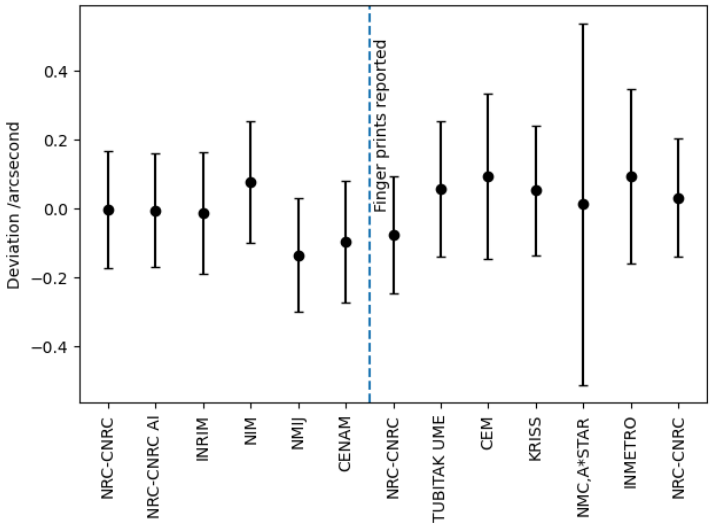

Figure 16: Angle 1:2 for polygon 327. Error bars are $U(k = 2)$ and have been expanded by the artifact instability.

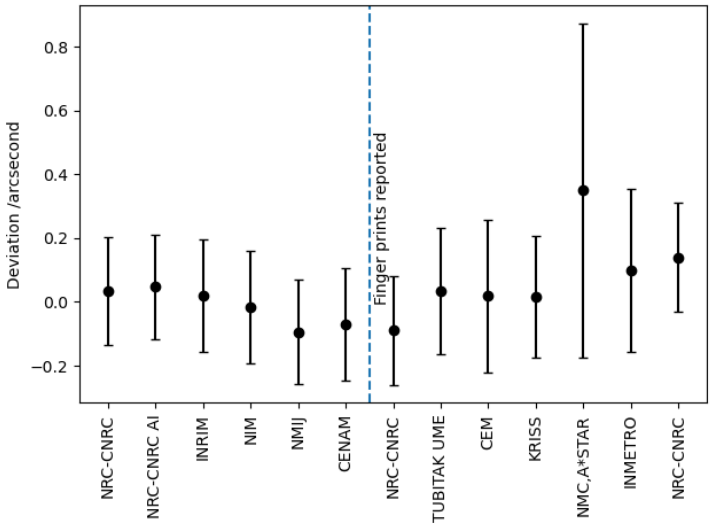

Figure 17: Angle 2:3 for polygon 327. Error bars are $U(k = 2)$ and have been expanded by the artifact instability.

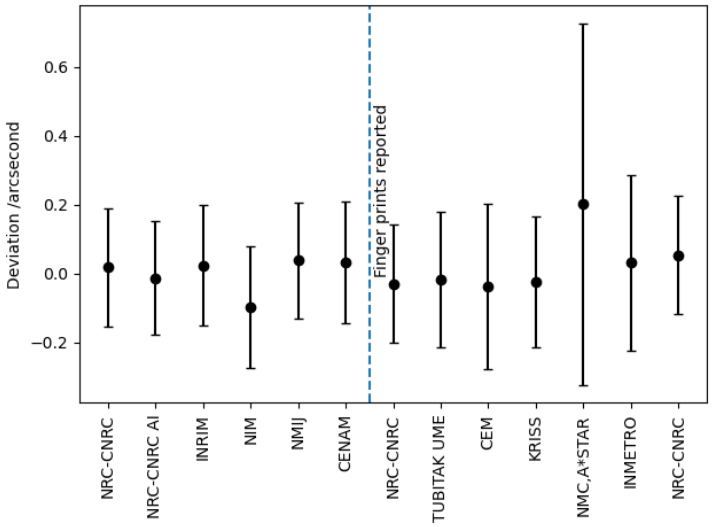

Figure 18: Angle 3:4 for polygon 327. Error bars are $U(k = 2)$ and have been expanded by the artifact instability.

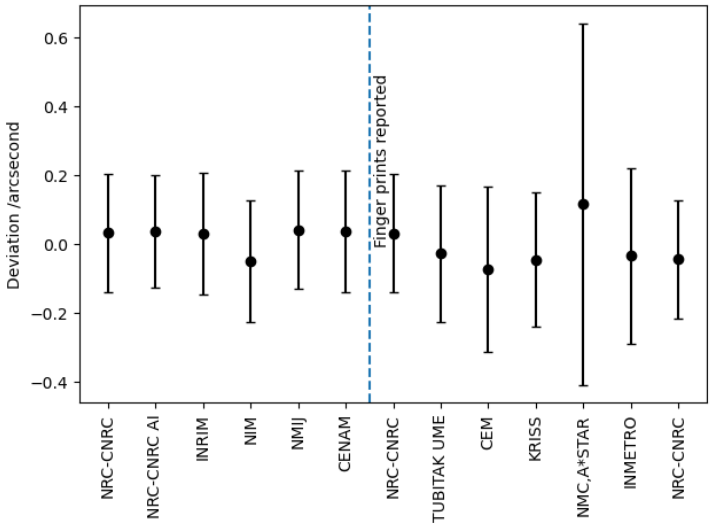

Figure 19: Angle 4:5 for polygon 327. Error bars are $U(k = 2)$ and have been expanded by the artifact instability.

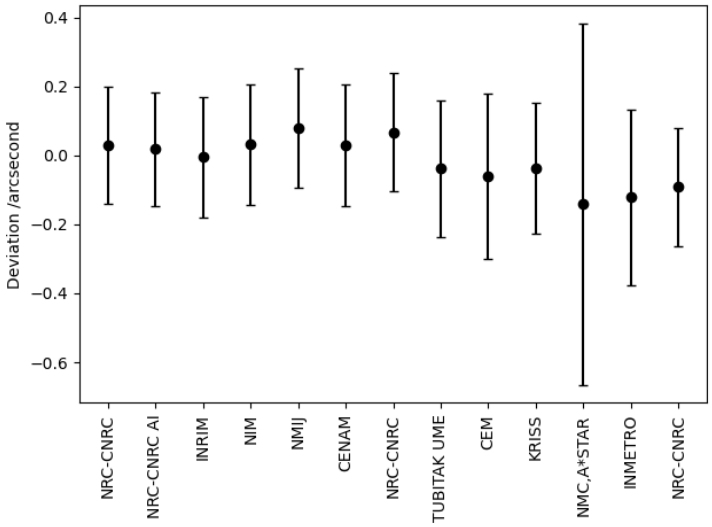

Figure 20: Angle 5:6 for polygon 327. Error bars are $U(k = 2)$ and have been expanded by the artifact instability.

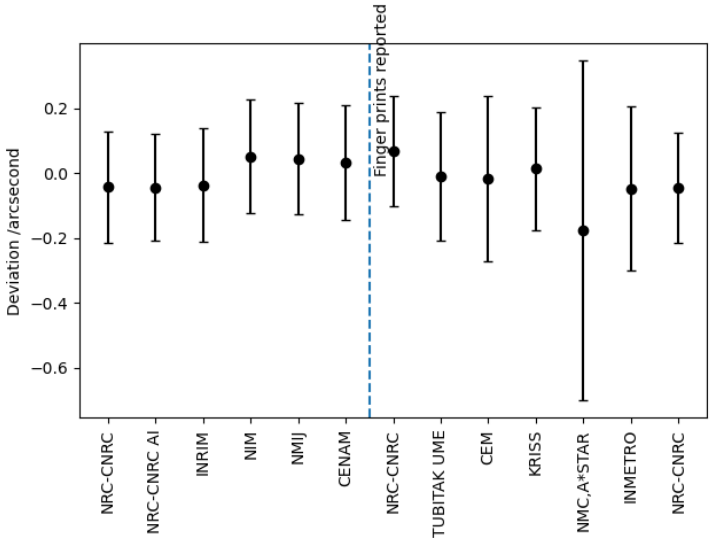

Figure 21: Angle 6:7 for polygon 327. Error bars are $U(k = 2)$ and have been expanded by the artifact instability.

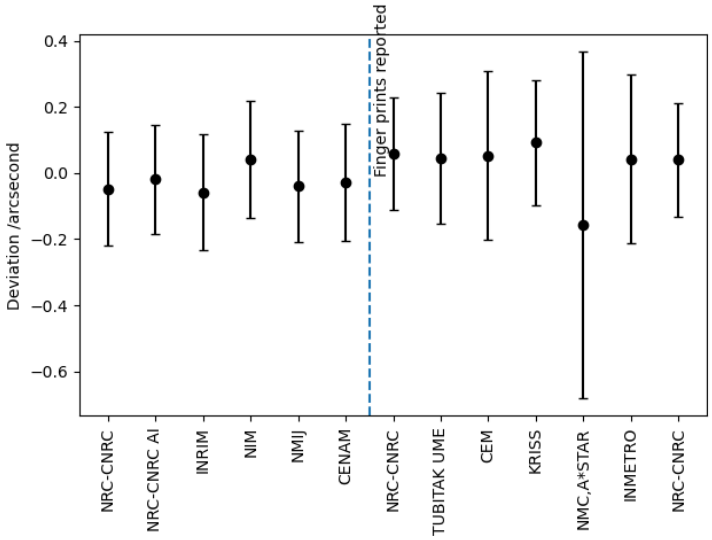

Figure 22: Angle 7:8 for polygon 327. Error bars are $U(k = 2)$ and have been expanded by the artifact instability.

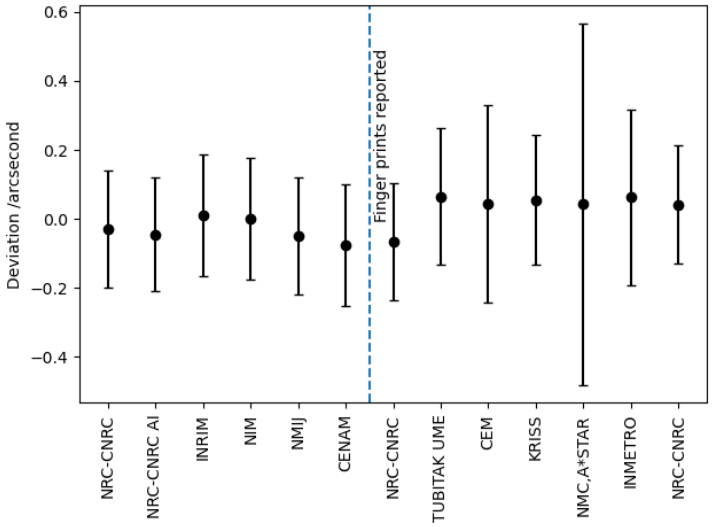

Figure 23: Angle 8:9 for polygon 327. Error bars are $U(k = 2)$ and have been expanded by the artifact instability.

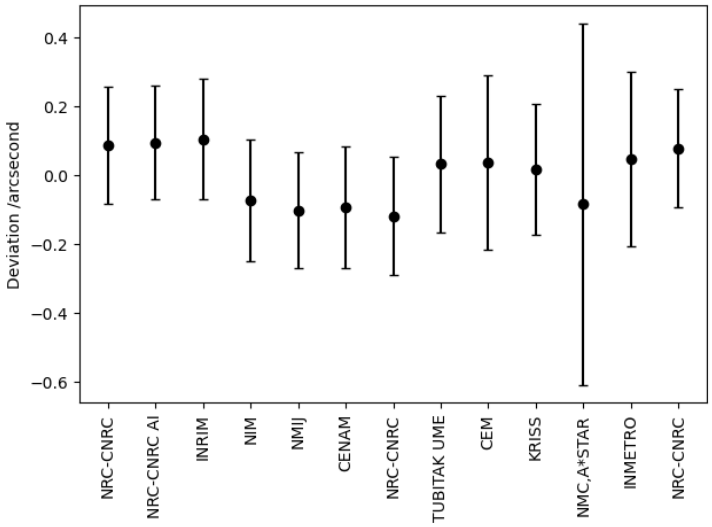

Figure 24: Angle 9:10 for polygon 327. Error bars are $U(k = 2)$ and have been expanded by the artifact instability.

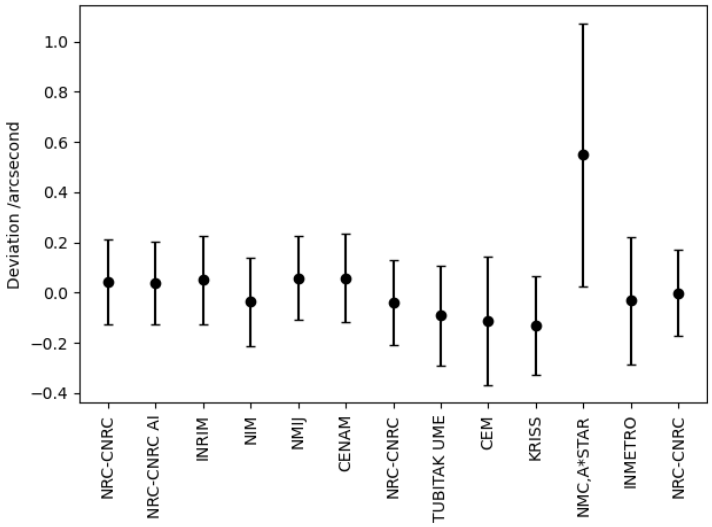

Figure 25: Angle 10:11 for polygon 327. Error bars are $U(k = 2)$ and have been expanded by the artifact instability.

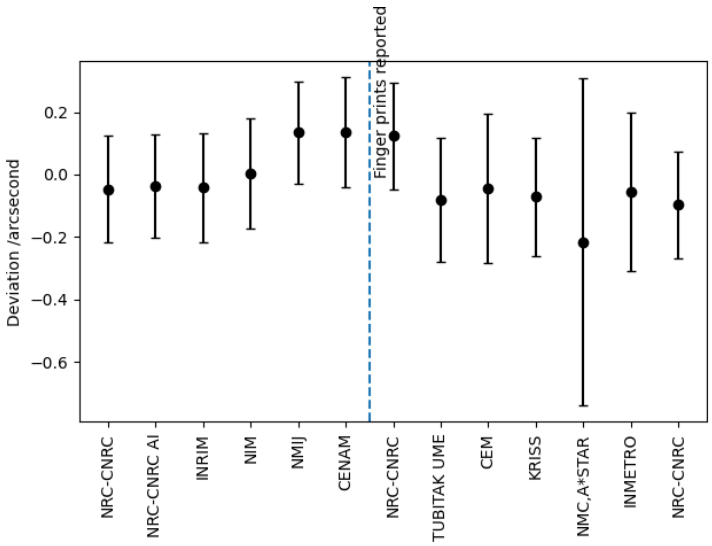

Figure 26: Angle 11:12 for polygon 327. Error bars are $U(k = 2)$ and have been expanded by the artifact instability.

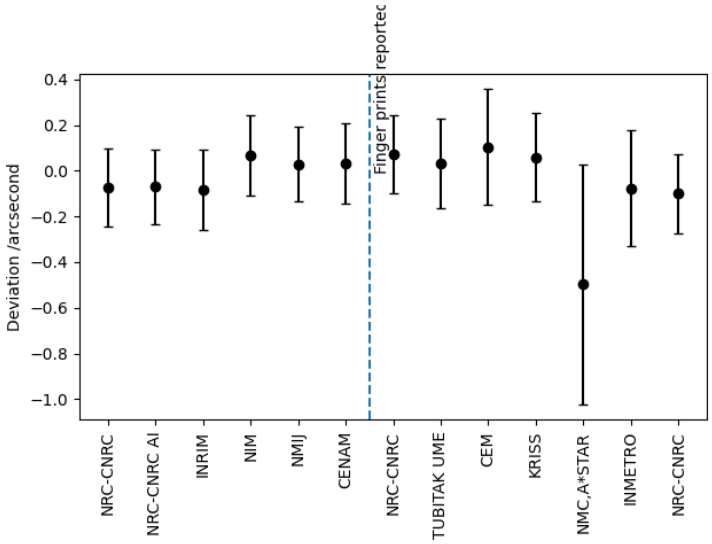

Figure 27: Angle 12:1 for polygon 327. Error bars are $U(k = 2)$ and have been expanded by the artifact instability.

polygon (stainless steel base supporting a low coefficient of thermal expansion glass polygon) and thermal cycling. The instability is large enough that the corresponding uncertainty contribution dominates for most participants and the results are not a good test of the participants' measurement capabilities.

7.5 Support of uncertainty claims

To provide guidance on whether a participants' results support their uncertainty claims we check whether all their measurements have normalised errors less than one, and whether the chi-squared test statistic

$$Q = \sum_{i=1}^{n} (k_i \cdot E_{ni})^2 \tag{12}$$

where k_i equals the coverage factor, is less than the 95^{th} percentile of the chi square distribution with M degrees of freedom. This is functionally equivalent to the Birge limit test but applied to all the measurands of a single participant. If either test is passed then the particpants' results are understood to be consistent with their uncertainty claims. If both tests fail then the participant should investigate further to see if there is a problem [3].

Since the angles of the polygon are constrained by the circle-closure relation the degrees of freedom for a polygon with n faces is simply $n - 1$. The total degrees of freedom for both polygons is, therefore, $M = 20$. Table 12 shows the results for both tests and whether any investigative action is required for any of

the participants. The only laboratory failing both tests is NMC,A*STAR. The uncertainty used by NMC,A*STAR for the 10-sided polygon measurement is smaller than their CMC uncertainty. If their CMC uncertainty is used instead then NMC,A*STAR passes the chi-squared test.

Table 12: Assessment of whether the participants results support their uncertainty claims.

NMI	$\|E_n\| > 1$	Q	$\chi^2_{20,0.95}$	Action
NRC-CNRC	0	5.8	31.4	
INRIM	0	5.6	31.4	
NIM	0	5.6	31.4	
NMIJ	0	13.1	31.4	
CENAM	0	8.9	31.4	
TUBITAK UME	0	4.2	31.4	
CEM	0	3.7	31.4	
KRISS	0	5.8	31.4	
NMC,A*STAR	3	34.7	31.4	investigate
INMETRO	0	9.1	31.4	

The service categories and CMCs supported by this comparison can be found by looking up the key comparison topic area, i.e. K3, in the CCL Competence Matrix.

A Appendix: Analysis of the 12-sided polygon without the artefact stability uncertainty

The analysis of the 12-sided polygon (serial number 327) is recalculated without the stability uncertainty component. The calculated reference values are shown in table 13, the E_n values are shown in table 14, and the differences between the participants' measurement results and the reference values are graphed in figures 28 through 39. The data clearly shows that the majority of comparison participants are unable to agree with the KCRV within their stated measurement uncertainties when the artefact stability uncertainty is excluded from the calculations. One could be tempted to group NMI measurements together into self-consistent steps based upon the measurement time line. Unfortunately a consistent grouping across all angles is not possible.

Table 13: Reference values for polygon 327 calculated without the additional stability uncertainty component. Units are in arcseconds.

Angle	Value	$U(k=1)$	R_B	R_B Limit
1:2	−0.333	0.013	2.08	1.39
2:3	−0.713	0.014	1.45	1.39
3:4	−0.478	0.015	1.05	1.39
4:5	−0.297	0.015	0.87	1.39
5:6	0.358	0.015	0.97	1.39
6:7	0.551	0.015	0.90	1.39
7:8	0.233	0.014	1.11	1.39
8:9	0.012	0.015	1.00	1.39
9:10	0.067	0.015	1.93	1.39
10:11	−0.588	0.014	1.58	1.39
11:12	0.250	0.014	2.22	1.39
12:1	0.929	0.014	1.56	1.39

Table 14: E_n values for the polygon with serial number 327 calculated without the additional stability uncertainty component. Reference values in table 13 used to calculate E_n values.

NMI	1:2	2:3	3:4	4:5	5:6	6:7
NRC-CNRC	0.60	0.97	0.24	0.39	0.22	−0.80
NRC-CNRC AI	0.64	1.29	−0.30	0.49	0.01	−0.85
INRIM	0.37	0.61	0.28	0.29	−0.31	−0.57
NIM	1.55	0.08	-1.37	−0.80	0.19	0.65
NMIJ	-2.53	-1.67	0.62	0.50	0.93	0.63
CENAM	−0.75	−0.62	0.38	0.36	0.16	0.39
NRC-CNRC	−0.52	−0.90	−0.46	0.30	0.69	0.90
TUBITAK UME	0.83	0.49	−0.18	−0.32	−0.47	−0.11
CEM	0.75	0.24	−0.24	−0.47	−0.44	−0.11
KRISS	0.90	0.40	−0.28	−0.49	−0.52	0.10
NMC,A*STAR	0.11	0.75	0.40	0.21	−0.32	−0.36
INMETRO	0.67	0.62	0.14	−0.22	−0.70	−0.26
NRC-CNRC	0.97	2.23	0.66	−0.72	-1.46	−0.66

NMI	7:8	8:9	9:10	10:11	11:12	12:1
NRC-CNRC	−0.56	−0.25	1.60	0.36	-1.35	-1.29
NRC-CNRC AI	−0.09	−0.53	1.80	0.34	-1.31	-1.31
INRIM	−0.61	0.35	1.54	0.41	-1.04	-1.18
NIM	0.73	0.22	−0.88	−0.75	−0.40	0.89
NMIJ	−0.52	−0.63	-1.66	0.86	2.52	0.68
CENAM	−0.18	−0.83	-1.16	0.50	1.33	0.41
NRC-CNRC	1.01	−0.72	-1.55	−0.83	1.24	0.96
TUBITAK UME	0.51	0.69	0.34	−0.96	−0.99	0.25
CEM	0.34	0.24	0.22	−0.67	−0.45	0.51
KRISS	1.04	0.70	0.23	-1.30	-1.02	0.52
NMC,A*STAR	−0.29	0.12	−0.15	1.06	−0.50	-1.00
INMETRO	0.29	0.40	0.27	−0.26	−0.46	−0.40
NRC-CNRC	0.73	0.76	1.14	−0.30	-1.81	-1.41

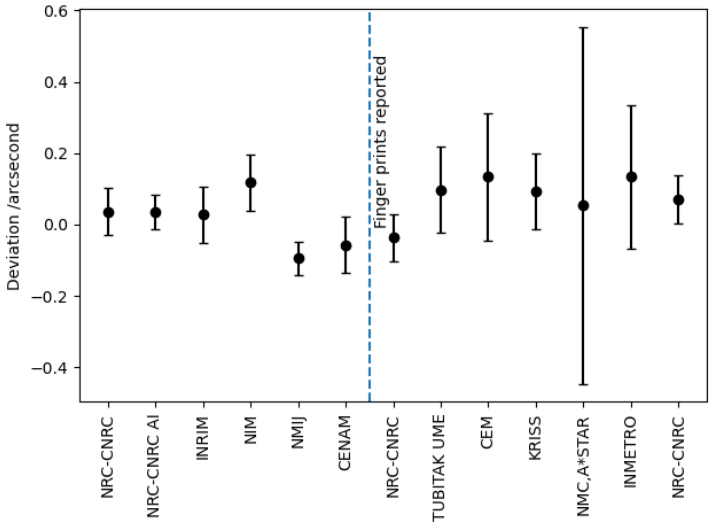

Figure 28: Angle 1:2 for polygon 327 without additional stability uncertainty component. Error bars are $U(k = 2)$.

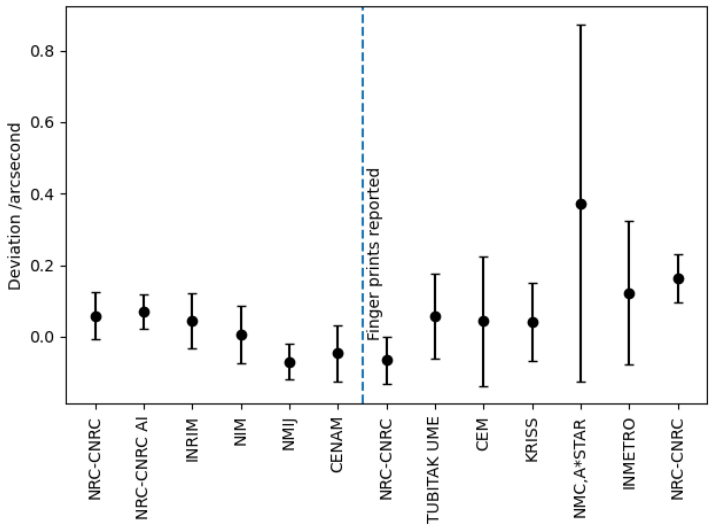

Figure 29: Angle 2:3 for polygon 327 without additional stability uncertainty component. Error bars are $U(k = 2)$.

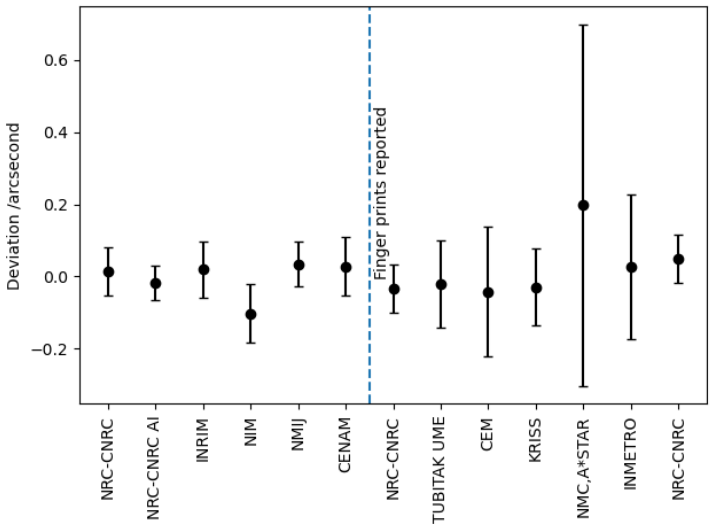

Figure 30: Angle 3:4 for polygon 327 without additional stability uncertainty component. Error bars are $U(k = 2)$.

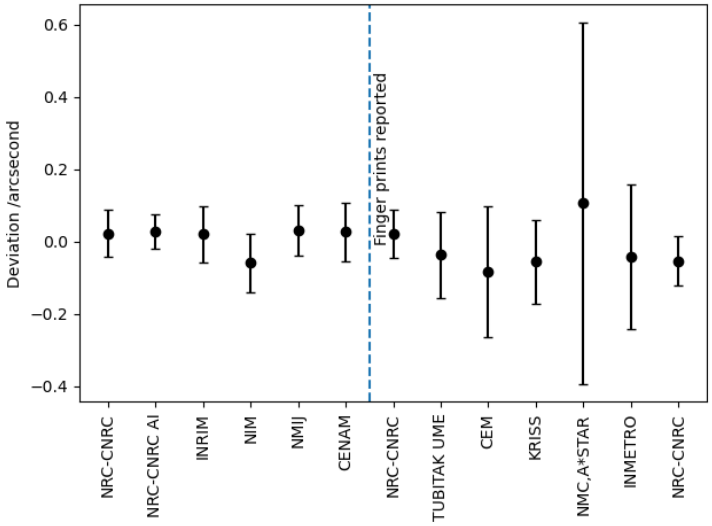

Figure 31: Angle 4:5 for polygon 327 without additional stability uncertainty component. Error bars are $U(k = 2)$.

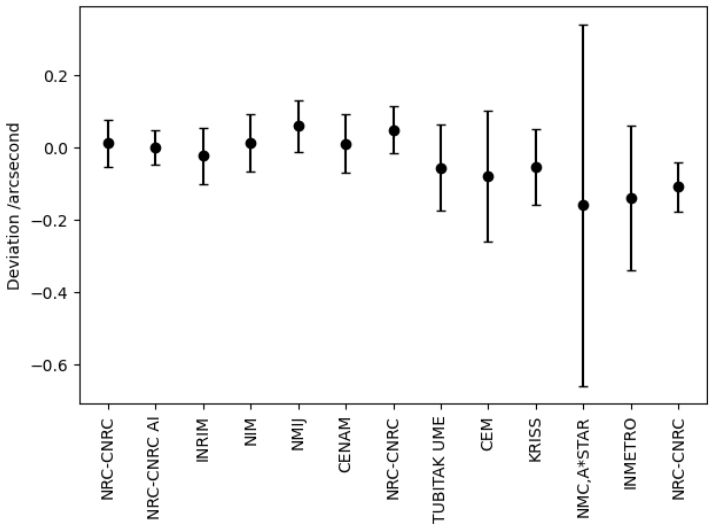

Figure 32: Angle 5:6 for polygon 327 without additional stability uncertainty component. Error bars are $U(k = 2)$.

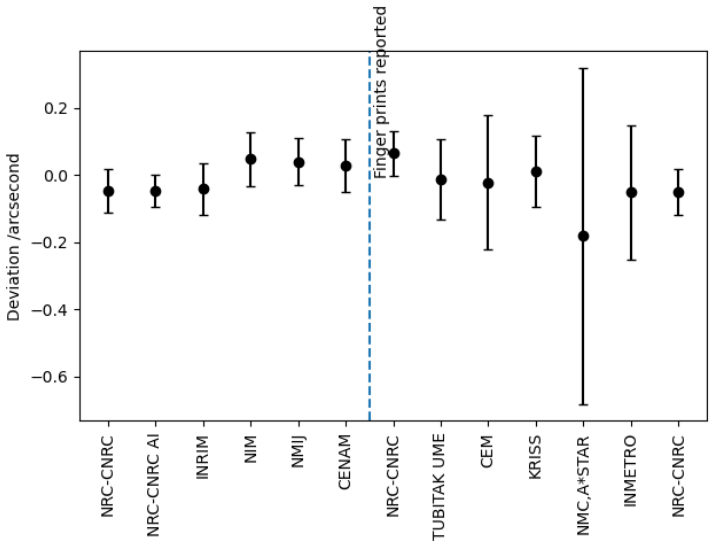

Figure 33: Angle 6:7 for polygon 327 without additional stability uncertainty component. Error bars are $U(k = 2)$.

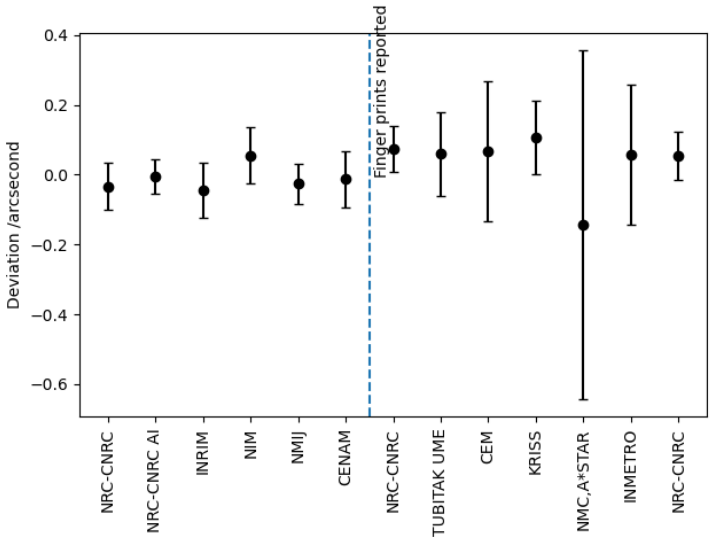

Figure 34: Angle 7:8 for polygon 327 without additional stability uncertainty component. Error bars are $U(k = 2)$.

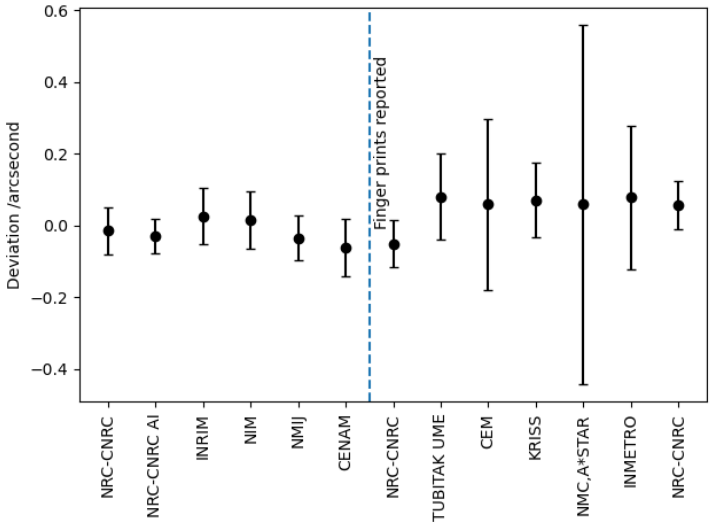

Figure 35: Angle 8:9 for polygon 327 without additional stability uncertainty component. Error bars are $U(k = 2)$.

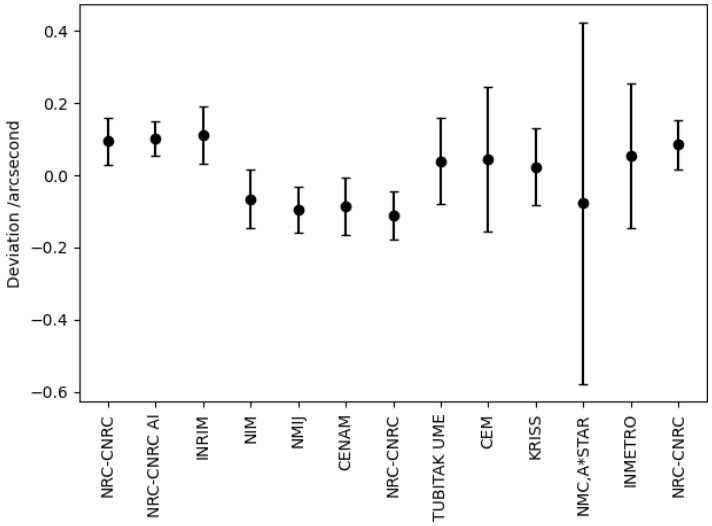

Figure 36: Angle 9:10 for polygon 327 without additional stability uncertainty component. Error bars are $U(k = 2)$.

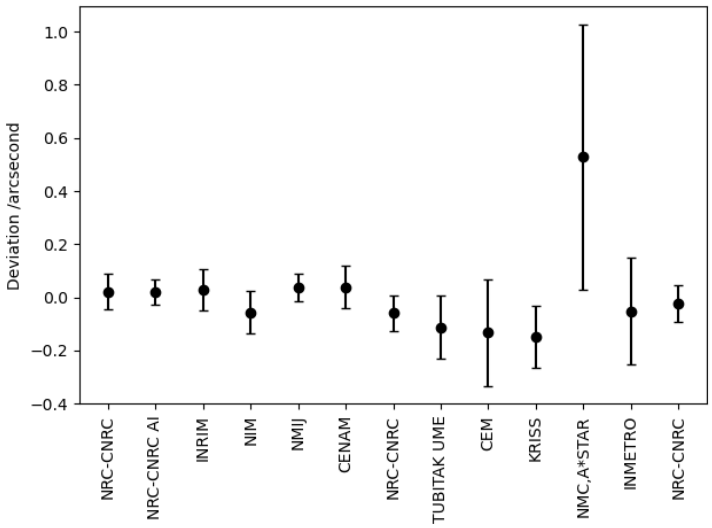

Figure 37: Angle 10:11 for polygon 327 without additional stability uncertainty component. Error bars are $U(k = 2)$.

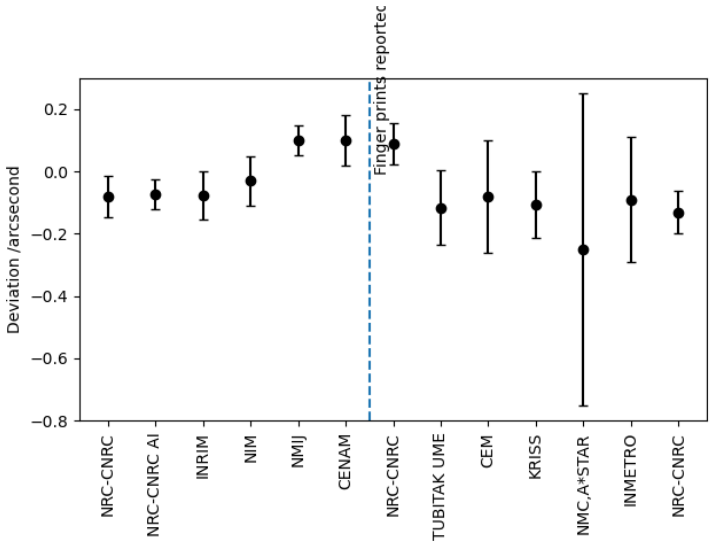

Figure 38: Angle 11:12 for polygon 327 without additional stability uncertainty component. Error bars are $U(k = 2)$.

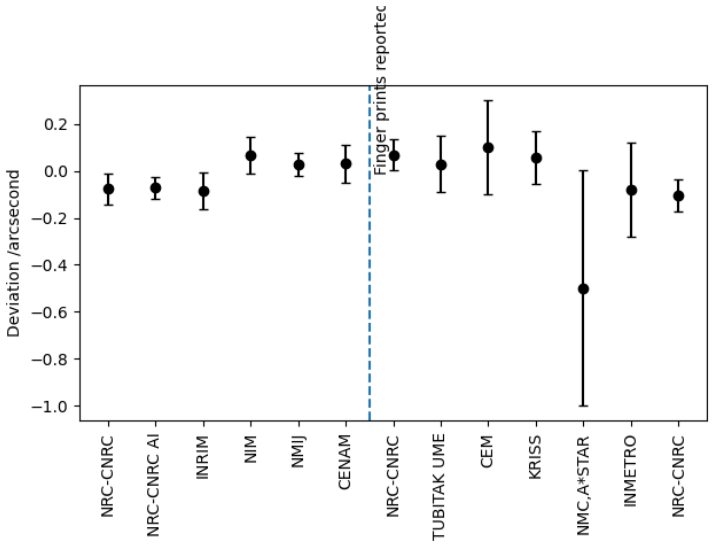

Figure 39: Angle 12:1 for polygon 327 without additional stability uncertainty component. Error bars are $U(k = 2)$.

B Appendix: Surface form

The surface topographies of the measurement faces of the 10-sided polygon (serial number 31391.15) and the 12-sided polygon (serial number 327) are shown in figures 40 and 41. The topography images were generated using the angle interferometer at NRC-CNRC [4].

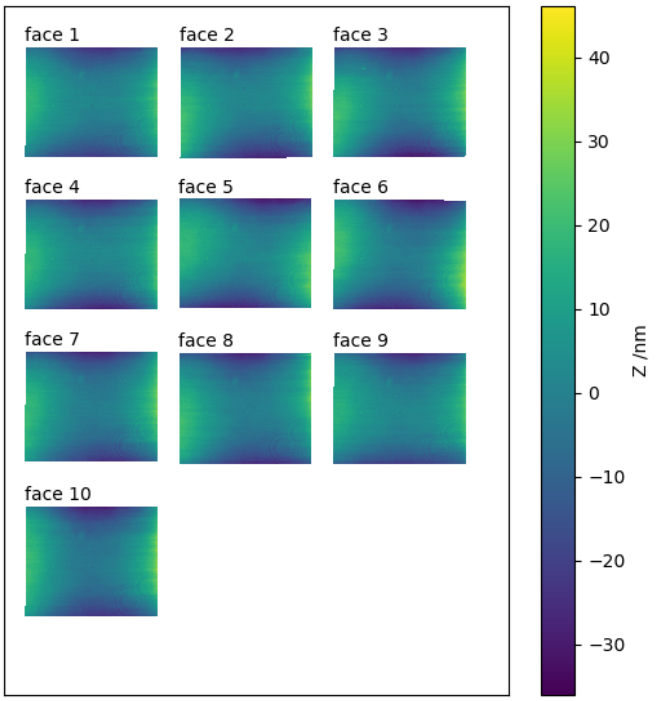

Figure 40: Surface form for the faces of the 10-sided polygon with serial number 31391.15.

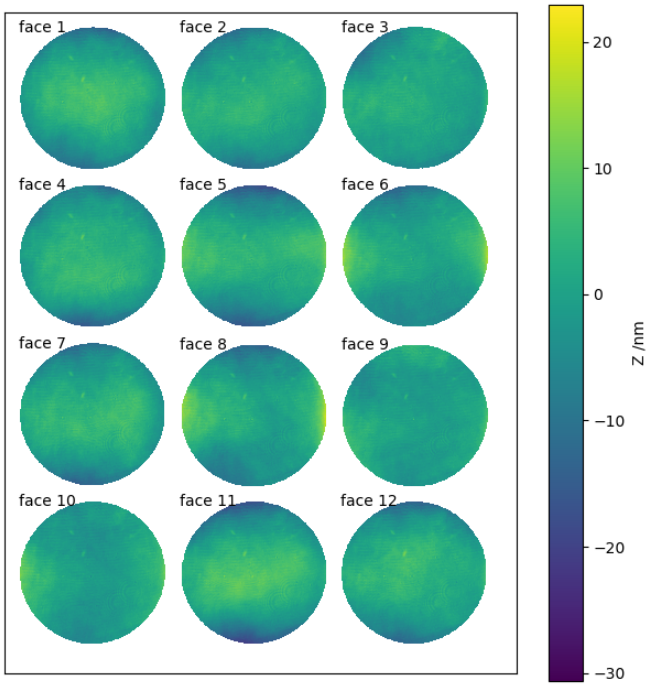

Figure 41: Surface form for the faces of the 12-sided polygon with serial number 327.

References

[1] Beissner K. On a measure of consistency in comparison measurements. *Metrologia*, 39:59, 2002.

[2] Decker J.E., Brown N., Cox M.G., Steele A.G., and Douglas R.J. Recent recommendations of the consultative committee for length (ccl) regarding strategies for evaluating key comparison data. *Metrologia*, 43, 2006.

[3] CCL guidance document GD-3: Guide to preparation of key comparison reports in dimensional metrology.

[4] B J Eves, I D Leroux, and A J Cen. Phase shifting angle interferometer. *Metrologia*, 60:055006, 2023.